



Dating folding beyond folding, from layer-parallel shortening to fold tightening, using mesostructures: Lessons from the Apennines, Pyrenees and Rocky Mountains.

Olivier Lacombe¹, Nicolas E. Beaudoin², Guilhem Hoareau², Aurélie Labeur², Christophe Pecheyran³,

5 Jean-Paul Callot²

¹ Sorbonne Université, CNRS, Institut des Sciences de la Terre de Paris, Paris, France

² Université de Pau et des Pays de l'Adour, E2S UPPA, CNRS-TOTAL, LFCR, Pau, France

³ Université de Pau et des Pays de l'Adour, E2S UPPA, IPREM, Pau, France

10 *Correspondence to:* Olivier Lacombe (olivier.lacombe@sorbonne-universite.fr)

Abstract. Dating syntectonic sedimentary sequences is often seen as the unique way to constrain the initiation, kinematics and rate of folding and the sequence of deformation in the shallow crust. Beyond fold growth however, deformation mesostructures accommodate the internal shortening of pre-folding strata before, during and after strata tilting. Absolute dating of mesostructures developed during extension at fold hinge may help constrain the duration of fold growth in the absence of preserved growth strata, while dating of mesostructures related to layer-parallel shortening and late fold tightening provide a valuable access to the timing and duration of the entire folding event. We compile existing ages in the literature and provide new U-Pb ages of calcite cements from veins and faults from four folds (Apennines, Pyrenees, Rocky Mountains). Our results not only better constrain the timing of fold growth but also reveal a contraction preceding and following folding, the duration of which might be function of the tectonic style and regional sequence of deformation. This study paves the way for a better appraisal of folding lifetime and processes and of stress evolution in folded domains.

1 Introduction

Quantifying the rates and duration of deformation processes is key to understand how the continental crust deforms. Quite a lot is known about rates and duration of ductile deformation in the lower crust, for instance that



25 shear zones can be active for 10s or 100s My (Schneider et al., 2013; Mottram et al., 2015). However, little is known about the duration and rates of folding processes in the upper crust. Short-term folding rates are usually captured by studying deformed terraces and alluvial fan ridges associated with active folds, and the dating of the inception and lifetime of folds is based on the extrapolation of these short-term rates back in time assuming a steady deformation rate.

30 The other classical mean to constrain the age and rate of upper crustal folding consists in dating growth strata. In orogenic forelands, contractional deformation causes folding of the pre-deformational sedimentary sequence and when sedimentation occurs continuously during deformation, growth strata are deposited synchronously with folding. Growth strata often show a characteristic pattern, such as decreasing dips up section toward the limbs of the fold, fan-like geometry and unconformities (Riba, 1976; Fig.1). Several factors control
35 growth strata patterns, such as kink-band migration, fold uplift, limb rotation and lengthening rates, as well as sedimentation and erosion rates (Suppe et al., 1992; Storti and Poblet, 1997). Chronostratigraphic constraints are critical for defining the duration and rate of fold growth (Butler and Lickorish, 1997). Dating the base of the growth strata defines the youngest initiation age for the fold, while post-growth strata conceal the final geometry of the fold and mark the end of folding (Fig.1).

40 However, fold growth may be highly discontinuous through time, deformation being episodic at all time scales with tectonic uplift pulses of different duration and intensity interrupted by periods of variable extent in which no fold growth occurred, rather than occurring in a continuum (Masferro et al., 2002; Carrigan et al., 2016; Anastasio et al., 2018). The study of syntectonic unconformities (Barnes, 1996) or terraces (Mueller and Suppe, 1997) otherwise suggest that the growth of some folds may be caused by earthquake-related slip on active faults,
45 which is by essence discontinuous. These studies emphasize the difficulty to extrapolate fold growth rates back in time. The age of fold initiation obtained by assuming steady shortening rate, deposition rate and fold growth rate is therefore at best strongly biased, at worst false, so the duration of fold growth remains poorly constrained.



Folding is also accompanied by deformation mesostructures such as faults, joints and veins, and stylolites (e.g. Tavani et al., 2015, and references therein) which accommodate the internal **shortening** of strata during 50 folding, but also before strata started to be tilted and after tilting when shortening can no longer be accommodated by fold growth (Fig.1). Several deformation stages can typically be identified in folded pre-compressional strata, starting with pre-shortening extension related to foreland flexure and bulging, followed by layer-parallel shortening (LPS, horizontal shortening of flat-lying strata) (Amrouch et al., 2010a; Callot et al., 2010; Lacombe et al., 2011; Tavani et al., 2006, **2008**, 2011; Rocher et al., 2000; Beaudoin et al., 2012, 2016; Branellec et al., 2015). Continuing 55 horizontal stress loading and shortening usually leads to folding, associated with strata tilting and curvature and accommodated by flexural slip and **outer arc extension in the fold hinge**. The fold ‘locks’ when limb rotation and/or kink-band migration cannot accommodate shortening anymore. At that stage, strata tilting is over but continuous horizontal shortening leads to late stage fold tightening (LSFT), accommodated by late mesostructures developing irrespective of bedding dip (Fig. 1) (Amrouch et al., 2010a; Tavani et al., 2015). Yet, despite recent efforts (Wang 60 et al., 2016; Curzi et al., 2020), the dating of the early-, syn- and late-folding mesostructures has received poor attention, although it is key to constrain not only the absolute timing of folding in the absence of growth strata, but also the entire duration of the fold-related contractional stages and the associated stress evolution from build-up to release.

We explore hereinafter the possibility to define the age and duration of folding by investigating how and 65 for how long pre-folding strata have been accommodating shortening from the onset to the end of the horizontal contraction from which the fold originated, an event we define as the folding event (Fig. 1). This approach will better constrain the duration of fold growth by dating the syn-folding mesostructures, but also by bracketing fold growth age by dating mesostructures that immediately predate and postdate strata tilting. Doing so also enables to capture the duration of the LPS and LSFT, two stages which have been overlooked since they accommodate much 70 less shortening than folding itself, while being key periods of time for large scale fluid flow and related ore



deposition in fold-thrust belts and sedimentary basins (e.g., Roure et al., 2005; Evans and Fischer, 2012; Beaudoin et al., 2014). For this purpose, we consider four natural folds for which we either compile existing data or provide new estimates of the age of LPS, fold growth and LSFT. Three of our examples are from fold-and-thrust belts (Apennines, Pyrenees), and one from the Laramide basement-cored folding province (Rocky Mountains). We show
75 that mesostructures can be used to constrain the timing and duration of fold growth and/or of shortening preceding and following folding. Our results not only provide new estimates of the duration of folding, but also establish that the overall duration of the folding event may strongly vary as a function of the tectonic style of deformation, paving the way to a better mechanical appraisal of contractional deformation and stress evolution in folded domains.

80 **2 Methods for dating the folding event using mesostructures**

In this paper, we focus on easily recognizable mesostructures that develop in the same contractional stage and under the same regional trend of horizontal shortening than folding. We do not report hereinafter on microscale features (eg, calcite twins : Craddock et al., 1993; Lacombe et al., 2007, 2009; Rocher et al., 1996; Hnat et al., 2011; see review by Lacombe, 2010) or rock physical properties such as anisotropy of magnetic susceptibility (e.g,
85 Aubourg et al., 2010; Amrouch et al., 2010b; Branellec et al., 2015, Weil and Yonkee, 2012) which have also been shown to be suitable recorders of the stress and strain history of folded strata (Lacombe et al., 2012) but the precise dating of which remains out of reach to date.

In the four examples of fold we investigated, the sequence and age of mesostructures were established by various dating approaches, of which methodologies are briefly recalled below (Fig.2). Note that strata from which
90 mesostructures were dated are mainly pre-folding strata, and that there has been few (if any) attempts at directly dating mesostructures that developed within growth strata reported in the literature. The reason **would be** that the often poorly indurated syn-folding formations are less prone to fracturing and calcite cementation at the time of deformation compared to pre-folding, well-indurated ~~carbonate~~ carbonate formations.



2.1 Sequence of mesostructures related to the fold history

95 The characterization of the sequence of deformation was based on field measurements of stylolites and fractures and their grouping into sets according to their statistical orientation, deformation mode and relative chronology established from abutting and crosscutting relationships (Fig.2A). Their timing with respect to fold growth (i.e., early, syn-, and late folding mesostructures) was further established by considering their current and unfolded attitude at fold hinge and limbs (eg., Beaudoin et al, 2012, 2016; Tavani et al., 2015) (Fig.1).

100 Field observations (eg., Bellahsen et al., 2006; Ahmadhadi et al., 2008; Tavani et al., 2015) and numerical modelling (Guiton et al., 2003; Sassi et al., 2012) have emphasized the widespread reactivation during folding of fractures formed during pre-folding stages. The role of reactivation should not be, and has not been, overlooked in our study; however, for the sake of reliable absolute dating we focused on fractures the characteristics of which support that they newly formed at each deformation stage and show no textural or petrographic evidence of multiple
105 opening or shearing events.

2.2 Dating veins and faults

Calcite-bearing veins and faults can be dated by combining the absolute precipitation temperature of the fluids from which calcite cements formed as given by carbonate clumped isotope Δ_{47} thermometry with the burial-time history of strata ~~derived from well data~~ (Fig.2B). Provided that (1) cementation was nearly coeval with fracturing, (2) the
110 geotherm can be reliably estimated and (3) stable isotope geochemistry points towards fluid precipitation at thermal equilibrium with the host, clumped isotope thermometry of cements combined to strata burial history yields the absolute timing of the successive vein sets, hence the timing of the related deformation stages (Fig.2D) (Labeur et al., 2021).

Calcite cements can also be directly dated by carbonate geochronology (Fig.2B). Laser ablation–
115 inductively coupled plasma–mass spectrometry (LA-ICP-MS) U-Pb dating of calcite consistently reveals the age of brittle deformation events (Roberts and Walker, 2016; Nuriel et al., 2017; Hansman et al., 2018; Beaudoin et al.,



2018; Roberts et al., 2020)(Figs.2B and 2D), provided that cementation was coeval with fracturing and that no later fluid infiltration and/or calcite recrystallization has occurred (Roberts et al., 2021).

2.3 Combining sedimentary stylolite roughness inversion for paleodepth and burial history to constrain the onset of LPS

120

The onset of LPS corresponds to the time at which the maximum principal stress σ_1 switched from being vertical and related to compaction and/or to foreland flexure extension to being horizontal in response to tectonic contraction (Beaudoin et al., 2020a). In order to constrain the timing of this switch, our approach relies on the capability of bedding-parallel, sedimentary stylolite to fossilize the magnitude of the vertical stress σ_1 at the time
125 dissolution stopped. Indeed, signal analysis (e.g. wavelets) of the final roughness of a sedimentary stylolite returns scale-dependent power laws, of which the transition length (crossover length L_c) scales with the magnitude of the vertical stress σ_1 (Schmittbuhl et al, 2004; Toussaint et al., 2018) (Fig.2C). By analyzing a population of sedimentary stylolites with this inversion technique which has been validated in numerous studies (Ebner et al., 2009; Rolland et al., 2014; Bertotti et al., 2017; Beaudoin et al., 2016, 2019, 2020a,b), one can estimate the
130 maximum burial depth at which pressure solution was active, with 12% uncertainty (Rolland et al., 2014). Comparing this depth with the burial-time evolution of the strata as derived from **well data** provides access to the time at which compaction-driven pressure solution halted in the rock because of the switch of the maximum principal stress σ_1 from vertical to horizontal, thus revealing the age of the onset of LPS (Fig. 2D). The validity of such an approach has been established by the comparison of the age of the onset of LPS determined this way to the
135 oldest U-Pb absolute age of LPS-related cemented fractures (Beaudoin et al., 2020a).

3 Dating natural folding events

3.1 Cingoli and San Vicino Anticlines (Apennines)



The San Vicino and Cingoli anticlines belong to the Umbria-Marche Apennine Ridge (UMAR, Fig. 3A).
140 Apenninic deformation occurred by the Tortonian in the west of UMAR to the late Messinian-early Pliocene in the
east, reaching the Adriatic domain in the late Pliocene-Pleistocene (Calamita et al., 1994). UMAR undergoes post-
orogenic extension since ~3 Ma, being younger eastward and marked by recent or active normal faults cutting
through the nappe stack (Barchi, 2010). The San Vicino and the Cingoli anticlines involve platform carbonates
overlain by hemipelagic succession detached above Triassic evaporites and formed in late Messinian-early Pliocene
145 (~6-5 Ma) as indicated by growth strata in the nearby Aliforni syncline (Fig.3B), following a period of foreland
flexure-related extension marked by pre-contractual normal faults associated with turbidite deposition lasting
until early Messinian (~6.5 Ma) (Calamita et al., 1994; Mazzoli et al., 2002).

Field analysis in the Cingoli and San Vicino fault-bend anticlines (Fig.3B) has revealed three main sets of
mesostructures (Beaudoin et al., 2020b; Labeur et al., 2021). Set I consists in ~~vertical~~ veins perpendicular to both
150 bedding and fold axis and striking NE-SW, associated with bed-perpendicular tectonic stylolites with peaks striking
NE-SW and dipping parallel to bedding dip which, after unfolding, indicates NE-SW-directed LPS. Set II veins
are bed-perpendicular and strike NW-SE, parallel to the fold axis; they abut or cut across set I veins and formed in
response to outer-arc extension at fold hinge. Set III comprises NE-SW striking vertical veins closely associated
with vertical tectonic stylolites with horizontal peaks striking NE-SW and with conjugate vertical strike-slip faults
155 which formed during a post-tilting horizontal NE-SW contraction, i.e., LSFT (Fig.3C).

Labeur et al (2021) focused on the Cingoli anticline to reconstruct the burial history of the early Cretaceous
Maiolica Fm and Paleocene Scaglia Rossa carried out an extensive inversion of the roughness of sedimentary
stylolites from these formations to constrain the maximum depth at which compaction-related dissolution was
active. The results are shown in Fig.3D, together with the timing of veins from sets I and II as deduced from Δ_{47}
160 thermometry (Labeur et al., 2021) by considering a 23°C/km geotherm (Caricchi et al. 2015) and a 10°C surface
temperature. The resulting timing for LPS, fold growth and LSFT is shown in Fig.3F.



To extend the published dataset to the San Vicino Anticline, veins from sets I, II and III were sampled in the Cretaceous Maiolica Fm to perform U-Pb analyses for absolute dating. Selected veins display antitaxial, elongated-blocky or blocky textures (Bons et al., 2012) ensuring that the cements precipitated during, or soon after, vein opening. Cathodoluminescence observations further support the homogeneity of the cements (Fig.4) as well as the absence of any vein re-opening and calcite recrystallization or fluid infiltration that might cause anomalous younger (reset) ages (Roberts et al., 2021). U-Pb dating of calcite cements was conducted using LA-ICP-MS at the Institut des Sciences Analytiques et de Physico-Chimie pour l'Environnement et les Matériaux (IPREM) laboratory (Pau, France). Ages were determined from the total-Pb/U-Th algorithm of Vermeesch (2020), are quoted at 95% confidence, and include propagation of systematic uncertainties. Sample information, detailed methodology and results are provided in the Supplemental Material. Three veins from the San Vicino anticline yielded reliable ages: 6.1 ± 2 Ma for the set I vein, 3.5 ± 1 Ma for the set II vein and 3.7 ± 0.3 Ma for the set III vein (Fig. 3E). The large uncertainties on the U-Pb age from the set II vein lead to some overlap with the dates of set I and set III veins (Fig.3F). However, these veins have not only distinctive orientations and consistent relative chronology, but they also have distinctive C and O stable isotopic signatures of their cements while being sampled in the same part of the fold (Beaudoin et al., 2020b), which supports that these veins were not cemented by the same fluid, hence were not cemented coevally. The absolute vein ages, combined with existing time constraints (Fig.3F), indicate that LPS occurred from ~6.5 to 5.5 Ma for both anticlines, followed by fold growth between ~5.5 and ~3.5 Ma, with a seemingly slightly longer duration in Cingoli than in San Vicino. LSFT started ~5 Ma in the Camerino syncline (Beaudoin et al., 2020b), ~4.5 Ma in San Vicino and ~3 Ma in Cingoli, and possibly lasted until the onset of post-orogenic extension in eastern UMAR (~2.5-2 Ma, Fig.3F). The entire folding event was thus very short, having lasted 3-4 My considering both anticlines as a whole (Fig.3F).

3.2 Pico del Aguila Anticline (Pyrenees)



185 The Pico del Aguila is a N160°E trending anticline in the southern Pyrenees (Fig. 5A), markedly oblique to the south-Pyrenean thrust front. It formed in response to Pyrenean thrusting and detachment folding above Triassic evaporites (Poblet and Hardy, 1995, Fig. 5B). Growth strata (Fig.5B) indicate that the fold developed by late Lutetian-Priabonian (~ 42-35 Ma, Hogan and Burbank, 1996), before it was passively tilted and transported southward over the Guarga basement thrust (Jolivet et al., 2007).

190 Beaudoin et al. (2015) investigated the fracturing history of the Pico del Aguila (Fig. 5C). Three sets of bed-perpendicular joints/veins, oriented N080°E, N060°E and N045°E from the oldest to the youngest as established from abutting/cross cutting relationships formed in progressively younger strata under a stable, far-field NE-SW shortening while the area was undergoing a vertical axis 30-40° clockwise rotation (Fig.5C). This rotation agrees with the Bartonian-Priabonian clockwise vertical-axis 15-50° rotation identified from
195 paleomagnetism (Pueyo et al., 2002). Field study also revealed later bed-perpendicular joints oriented N160°E and N-S trending normal faults related to local outer-arc extension during folding (Fig.5C). The fracturing history ends with the formation of N-S trending reverse faults and transpressional reactivation of earlier ENE trending joints reflecting LSFT under an E-W compression resulting from the local rotation of the regional NE-SW compression (Beaudoin et al., 2015), followed by post-folding E-W trending reverse faults that formed under the same late N-S
200 compression than the Guarga thrust (Fig.5C).

U-Pb dating of calcite cements reveals that the veins related to NE-SW directed LPS formed as early as ~61 ± 3 Ma ago, while late oblique-slip reverse faults (LSFT) and post-folding E-W reverse faults were dated 19 ± 5 Ma and 18-14 ± 3 Ma, respectively (Hoareau et al., 2021). LPS, folding and LSFT therefore lasted ~19 My (61-42 Ma), ~7 My (42-35 Ma) and ~17 My (35-18 Ma), respectively (Fig.5D).

205

3.3 Sheep Mountain Anticline (Rocky Mountains)



Sheep Mountain anticline is a thrust-related, basement-cored NW-SE striking fold that developed in the Bighorn basin (Figs. 6A and B) during the late Cretaceous-Paleogene Laramide contraction. Three main joint/vein sets were recognized (Fig. 6C, Bellahsen et al., 2006; Amrouch et al., 2010; Barbier et al., 2012). Set I consists in
210 bed-perpendicular, WNW-ESE oriented veins associated with tectonic stylolites with ~WNW-ESE horizontal peaks (after unfolding) (Amrouch et al., 2010a, 2011). This set formed prior to folding under an horizontal σ_1 striking WNW-ESE likely transmitted from the distant thin-skinned Sevier orogen at the time the Bighorn basin was still part of the Sevier undeformed foreland. Set II comprises vertical, bed-perpendicular joints/veins striking NE-SW, i.e., perpendicular to the fold axis. These veins are associated with tectonic stylolites with horizontal peaks
215 oriented NE-SW and witness a NE-SW directed LPS (Varga, 1993; Amrouch et al., 2010a; Weil and Yonkee, 2012). The joints/veins of set III are bed-perpendicular and abut or cut across the veins of the former sets. They strike NW-SE parallel to the fold axis and their distribution mainly at the hinge zone of the fold support that they developed during outer-arc extension at the hinge of the growing anticline (Fig.6C). Widespread reverse and strike-slip faults also formed during LPS and LSFT, while bedding-parallel slip surfaces developed during fold growth
220 (Amrouch et al., 2010a).

Veins from sets I, II and III were dated by means of U-Pb (Beaudoin et al., 2018). Set I veins yielded ages between 81 and 72 Ma, supporting their pre-Laramide formation. The Laramide LPS-related veins were dated 72–50 Ma. The age of set III veins constrains the timing of folding in the absence of preserved growth strata to 50–35 Ma (Beaudoin et al., 2018). Laramide LPS and fold growth therefore lasted ~20-25 My and ~15 My, respectively
225 (Fig. 6D). The duration of the LSFT is poorly constrained, being bracketed between 35 Ma and the onset of the Basin and Range extension and Yellowstone hot-spot activity at ~17 Ma (Camp et al., 2015, Fig. 6D).

4 Discussion and conclusion



Absolute dating of mesostructures definitely confirms the sequence of deformation usually deduced from
230 orientation data and relative chronology with respect to bedding attitude, and which includes LPS, fold growth
(e.g., strata tilting) and LSFT. This sequence is valid for the four folds studied, despite San Vicino, Cingoli and
Pico del Aguila anticlines developed above a decollement in a fold-and-thrust belt while Sheep Mountain anticline
formed as a basement-cored forced fold above a basement thrust. The overall consistency between ages of growth
strata when preserved, time constraints derived from our multi-proxy analysis coupling isotopic geochemistry of
235 cements and stylolite paleopiezometry, and U-Pb ages on early-, syn- and late-folding mesostructures demonstrates
the reliability of our approach. **Minor age overlaps are observed only when the duration of each deformation stage
was shorter than age uncertainties, i.e. in the case of recent and rapid deformation (San Vicino and Cingoli).**

Whatever the case, fold growth for the four folds lasted between 1.5 Ma and 15 Ma, in accordance with
previous estimates of fold growth duration elsewhere using either syntectonic sedimentation (Holl and Anastasio,
240 1993; Anastasio et al., 2018) or mechanical modeling (Yamato et al., 2011). Moreover, our study quantifies for the
first time the duration of the contraction before and after fold growth, and unexpectedly reveals that LPS and LSFT,
albeit associated with lower amounts of shortening but potentially to substantial - if not most of - small-scale rock
damage, may have lasted much longer than fold growth itself. Such trend can be key for the understanding of the
history of foreland basins, including strata mechanical evolution and past fluid flow dynamics (Roure et al., 2005;
245 Beaudoin et al., 2014).

Dating precisely the onset of LPS, whatever the technique used (U-Pb geochronology or absolute
thermometry of calcite cements of mesostructures) is difficult as the entire range of vein ages may not be captured
with certainty due to limited sampling. However, the onset of LPS can also be further constrained either by the
sedimentary record of the foreland flexure preceding contraction (San Vicino) or by the estimate of the time at
250 which vertical compaction-related pressure solution along bedding-parallel stylolites halted in the rocks in response
to the switch of σ_1 axis from vertical to horizontal (Cingoli). The end of LSFT is also difficult to constrain precisely,



but an upper bound is given by the change from fold-related shortening to a new regional state of stress. The latter is illustrated by the onset of post-orogenic extension in eastern UMAR (Fig.3), by the late Pyrenean compression in the Pico del Aguila area (Fig. 5) and by the Basin and Range extension in the Laramide province (Fig.6).

255 **The four examples of folds also show that the overall duration of the folding event is variable.** Fold growth lasted longer in the case of forced folding above a high angle basement thrust (Sheep Mountain) compared to fault-bend folding (San Vicino and Cingoli) along a flat-ramp decollement and detachment folding (Pico del Aguila) above a weak detachment layer in the cover (Fig. 4). The rapid fold growth and the relatively short LSFT in San Vicino and Cingoli are in line with the high rates of contraction and migration of deformation in the Apennines
260 (Calamita et al., 1994, Fig .7). In contrast, LSFT appears longer when folding is anchored to a high angle basement thrust or when the fold is located at the front of the orogenic wedge, i.e., when the later propagation of deformation is limited or slow, or when it occurs in a complex sequence (Pico del Aguila and Sheep Mountain, Fig.7). The duration of LPS reflects to some degree the duration of the stress/strain accumulation in rocks required to generate folding, which can depend on the structural style (Beaudoin et al., 2020c). Our results support that a longer LPS
265 (and a higher level of differential stress as well) is required to cause the inversion of a high angle basement normal fault and related forced folding of the undetached sedimentary cover (Sheep Mountain) than to initiate folding of the cover above a weak decollement (Pico del Aguila, Cingoli and San Vicino, Fig. 7). The longer LPS at Pico del Aguila compared to San Vicino and Cingoli (Fig.7) likely reflects the longer accumulation of displacement required to initiate folding oblique to the regional compression rather than perpendicular to it.

270 In summary, beyond regional implications, this study demonstrates that pre-, syn- and post-tilting mesostructures that formed under the same contraction than folding can be successfully dated. Our results bring for the first time absolute time constraints on the age and duration on the entire folding event for several upper crustal folds formed in different contractional settings. In particular, we not only better constrain the age and duration of fold growth, but also the onset and duration of the layer-parallel shortening stage that predates folding,



275 and the duration and end of the late stage fold tightening. Because the duration of fold growth as well as of the
early- and late folding shortening are found to depend on structural style and regional sequence of deformation, our
results emphasize the need to more carefully consider the entire folding event for a better appraisal of folding
processes and stress/strain evolution in orogenic forelands, and for a more accurate prediction of host rock damage
in naturally fractured reservoirs in folded domains.

280

Acknowledgements

NB is funded through the ISITE program E2S, supported by ANR PIA and Region Nouvelle- Aquitaine.

The authors thank Fabrizio Storti, Catherine Mottram and Stephen Marshak for their comments on an earlier
version of the manuscript.

285 References

- Ahmadhadi, F., Daniel, J.M., Azzizadeh, M. and Lacombe, O.: Evidence for pre-folding vein development in the
Oligo-Miocene Asmari Formation in the Central Zagros Fold Belt, Iran, *Tectonics*, 27, 2008.
- Amrouch, K., Lacombe, O., Bellahsen, N., Daniel, J. M. and Callot, J.P.: Stress and strain patterns, kinematics and
deformation mechanisms in a basementcored anticline: Sheep Mountain Anticline, Wyoming, *Tectonics*, 29(1),
290 TC1005, 2010a.
- Amrouch, K., Robion, P., Callot, J. P., Lacombe, O., Daniel, J. M., Bellahsen, N. and Faure, J. L.: Constraints on
deformation mechanisms during folding provided by rock physical properties: a case study at Sheep Mountain
anticline (Wyoming, USA), *Geophysical Journal International*, 182(3), 1105-1123, 2010b.
- Amrouch, K., Beaudoin, N., Lacombe, O., Bellahsen, N. and Daniel, J.M.: Paleostress magnitudes in folded
295 sedimentary rocks, *Geophys.Res. Lett.*, 38, L17301, 2011.
- Anastasio, D., Kodama, K., Parés, J.: 2018. Episodic deformation rates recovered from growth strata, Pyrenees,
Search and Discovery Article, 30553, 2018.



- Aubourg, C., Smith, B., Eshraghi, A., Lacombe, O., Authemayou, C., Amrouch, K., Bellier O. and Mouthereau, F.: New magnetic fabric data and their comparison with palaeostress markers in the Western Fars Arc (Zagros, 300 Iran): tectonic implications, *Geological Society London Special Publications*, 330(1), 97-120, 2010.
- Barbier, M., Leprêtre, R., Callot, J. P., Gasparrini, M., Daniel, J. M., Hamon, Y., Lacombe O. and Floquet, M.: Impact of fracture stratigraphy on the paleo-hydrogeology of the Madison Limestone in two basement-involved folds in the Bighorn basin (Wyoming, USA), *Tectonophysics*, 576, 116-132, 2012.
- Barchi, M.: The Neogene–Quaternary evolution of the Northern Apennines: crustal structure, style of deformation 305 and seismicity, *Journal of Virtual Explorer*, 36, 2010.
- Barnes P.M.: Active folding of Pleistocene unconformities on the edge of the Australian-Pacific plate boundary zone, offshore North Canterbury, New Zealand, *Tectonics*, 15, 623-640, 1996.
- Beaudoin, N., Leprêtre, R., Bellahsen, N., Lacombe, O., Amrouch, K., Callot, J.P., Emmanuel, L. and Daniel, J.M.: Structural and microstructural evolution of the Rattlesnake Mountain Anticline (Wyoming, USA): New insights 310 into the Sevier and Laramide orogenic stress build-up in the Bighorn Basin, *Tectonophysics*, 576-577, 20–45, 2012.
- Beaudoin, N., Koehn, D., Lacombe, O., Lecouty, A., Billi, A., Aharonov, E. and Parlangeau, C.: Fingerprinting stress: Stylolite and calcite twinning paleopiezometry revealing the complexity of progressive stress patterns during folding-The case of the Monte Nero anticline in the Apennines, Italy, *Tectonics*, 35, 1687-1712, 2016.
- Beaudoin, N., Lacombe, O., Roberts, N. M. W. and Koehn, D.: U-Pb dating of calcite veins reveals complex stress 315 evolution and thrust sequence in the Bighorn Basin, Wyoming, USA, *Geology*, 46, 1015-1018, 2018.
- Beaudoin, N., Huyghe, D., Bellahsen, N., Lacombe, O., Emmanuel, L., Mouthereau, F. and Ouahnon, L.: Fluid systems and fracture development during syn-depositional fold growth: example from the Pico del Aguila Anticline, Sierras Exteriores, Southern Pyrenees, Spain, *Journal of Structural Geology*, 70, 23-38, 2015.
- Beaudoin, N., Lacombe, O., David, M.E., Koehn, D.: Does stress transmission in forelands depend on structural 320 style? Distinctive stress magnitudes during Sevier thin-skinned and Laramide thick-skinned layer-parallel shortening in the Bighorn Basin (USA) revealed by stylolite and calcite twinning paleopiezometry, *Terra Nova*, 32, 225-233, 2020b.
- Beaudoin, N., Labeur, A., Lacombe, O., Koehn, D., Billi, A., Hoareau, G., Boyce, A., John, C.M., Marchegiano, M., Roberts, N.M., Millar, I.L., Claverie, F., Pecheyran, C. and Callot, J.P.: Regional-scale paleofluid system across 325 the Tuscan Nappe - Umbria Marche Apennine Ridge (northern Apennines) as revealed by mesostructural and isotopic analyses of stylolite-vein networks, *Solid Earth*, 11, 4, 1617-1641, 2020c.
- Beaudoin, N., Bellahsen, N., Lacombe, O., Emmanuel, L. and Pironon, J.: Crustal- scale fluid flow during the tectonic evolution of the Bighorn Basin (Wyoming, USA), *Basin Research*, 26(3), 403-435, 2014.



- Beaudoin N. E., Lacombe, O., Koehn, D., David, M.E., Farrell, N. and Healy, D.: Vertical stress history and
330 paleoburial in foreland basins unravelled by stylolite roughness paleopiezometry: Insights from bedding-parallel
stylolites in the Bighorn Basin, Wyoming, USA. *Journal of Structural Geology*. 136, 104061, 2020a.
- Bellahsen, N., Fiore, P. and Pollard, D. D.: The role of fractures in the structural interpretation of Sheep Mountain
Anticline, Wyoming, *Journal of Structural Geology*, 28, 850-867, 2006.
- Bertotti, G., de Graaf, S., Bisdorf, K., Oskam, B., Vonhof, H.B., Bezerra, F.H., Reijmer, J.G., and Cazarin, C.L.:
335 Fracturing and fluid-flow during post-rift subsidence in carbonates of the Jandaíra Formation, Potiguar Basin, NE
Brazil, *Basin Research*, 29, 836-853, 2017.
- Bons, P.D., Elburg, M.A. and Gomez-Rivas, E.: A review of the formation of tectonic veins and their
microstructures, *Journal of Structural Geology*, 43, 33–62, 2012.
- Branellec, M., Callot, J. P., Nivière, B. and Ringenbach, J. C.: The fracture network, a proxy for mesoscale
340 deformation: Constraints on layer parallel shortening history from the Malargüe fold and thrust belt, Argentina,
Tectonics, 34(4), 623-647, 2015.
- Butler, R.W.H. and Lickorish, W.H.: Using high-resolution stratigraphy to date fold and thrust activity: examples
from the Neogene of south-central Sicily, *Journal of the Geological Society*, 154, 633–643, 1997.
- Calamita, F., Cello, G., Deiana, G. and Paltrinieri, W.: Structural styles, chronology rates of deformation, and
345 time- space relationships in the Umbria- Marche thrust system (central Apennines, Italy), *Tectonics*, 13, 873-881,
1994.
- Callot, J.P., Robion, P., Sassi, W., Guiton, M.L.E., Kallel, N., Daniel, J.M., Mengus, J.M. and Schmitz, J.: Magnetic
characterisation of folded aeolian sandstones: interpretation of magnetic fabric in diamagnetic rocks,
Tectonophysics, 495, 230-245, 2010.
- 350 Camp V.E., Pierce K.L. and Morgan L.A. : Yellowstone plume trigger for Basin and Range extension, and coeval
emplacement of the Nevada–Columbia Basin magmatic belt, *Geosphere*, 1, 2; 203–225, 2015.
- Caricchi, C., Aldega, L. and Corrado, S.: Reconstruction of maximum burial along the Northern Apennines thrust
wedge (Italy) by indicators of thermal exposure and modeling, *Bull. Geol. Soc. Am.*, 127, 428–442, 2015.
- Carrigan, J.H., Anastasio D.J., Kodama K.P. and Parés J.M.: Fault-related fold kinematics recorded by terrestrial
355 growth strata, Sant Llorenç de Morunys, Pyrenees Mountains, NE Spain, *Journal of Structural Geology*, 91, 161-
176, 2016.
- Curzi, M., Aldega, L., Bernasconi, S. M., Berra, F., Billi, A., Boschi, C., Franchini S., Van der Lelij R, Viola G.
and Carminati, E.: Architecture and evolution of an extensionally-inverted thrust (Mt. Tancia Thrust, Central



- Apennines): Geological, structural, geochemical, and K–Ar geochronological constraints, *Journal of Structural Geology*, 136, 104059, 2020.
- 360 Craddock, J. P., Jackson, M., van der Pluijm, B. A. and Versical, R. T.: Regional shortening fabrics in eastern North America: Far- field stress transmission from the Appalachian-Ouachita Orogenic Belt, *Tectonics*, 12(1), 257-264, 1993.
- Ebner, M., Koehn, D., Toussaint, R., Renard, F. and Schmittbuhl, J. : Stress sensitivity of stylolite morphology, *Earth and Planetary Science Letters*, 277, 394-398, 2009.
- 365 Evans, M. A. and Fischer, M. P.: On the distribution of fluids in folds: A review of controlling factors and processes, *Journal of Structural Geology*, 44, 2-24, 2012.
- Guiton M.L., Sassi W., Leroy Y. and Gauthier B.D.: Mechanical constraints on the chronology of fracture activation in folded Devonian sandstones of the western Moroccan Anti-Atlas, *Journal of Structural Geology*, 25, 370 1317-1330, 2003.
- Hansman, R.J., Albert, R., Gerdes, A. and Ring, U.: Absolute ages of multiple generations of brittle structures by U-Pb dating of calcite, *Geology*, 46, 207–210, 2018.
- Hnat, J. S. and van der Pluijm, B. A.: Foreland signature of indenter tectonics: Insights from calcite twinning analysis in the Tennessee salient of the Southern Appalachians, USA, *Lithosphere*, 3(5), 317-327, 2011.
- 375 Hoareau, G., Crognier, N., Lacroix, B., Aubourg, C., Roberts, N.W., Niemi, N., Branellec, M., Beaudoin, N.E. and Suárez Ruiz, I.: Combination of $\Delta 47$ and U-Pb dating in tectonic calcite veins unravel the last pulses related to the Pyrenean shortening (Spain), *Earth and Planetary Science Letters*, 553, 116636, 2021.
- Hogan, P.J. and Burbank, D.W.: Evolution of the Jaca piggyback basin and emergence of the external Sierras, southern Pyrenees, In: Friend, P.F., Dabrio, C.J. (Eds.), *Tertiary Basins of Spain*. Cambridge Univ. Press, 153-160, 380 1996.
- Holl, J. E. and Anastasio, D. J.: Paleomagnetically derived folding rates, southern Pyrenees, Spain, *Geology*, 21, 271-274, 1993.
- Jolivet, M., Labaume, P., Monie, P., Brunel, M., Arnaud, N. and Campani, M.: Thermochronology constraints for the propagation sequence of the south Pyrenean basement thrust system (France-Spain), *Tectonics* 26, TC5007, 385 2007.
- Labeur, A., Beaudoin, N.E., Lacombe, O., Emmanuel, L., Petracchini, L., Daëron, M., Klimowicz, S. and Callot, J.-P.: Burial-deformation history of folded rocks unraveled by fracture analysis, stylolite paleopiezometry and vein cement geochemistry: A case study in the Cingoli Anticline (Umbria-Marche, Northern Apennines), *Geosciences*, 11, 135, 2021.



- 390 Lacombe, O., Bellahsen, N. and Mouthereau, F.: Fracture patterns in the Zagros Simply Folded Belt (Fars, Iran): constraints on early collisional tectonic history and role of basement faults, *Geological Magazine*, 148(5-6), 940-963, 2011.
- Lacombe, O., Amrouch, K., Mouthereau, F. and Dissez, L.: Calcite twinning constraints on late Neogene stress patterns and deformation mechanisms in the active Zagros collision belt, *Geology* 35, 263–266, 2007.
- 395 Lacombe, O., Malandain, J., Vilasi, N., Amrouch, K. and Roure, F.: From paleostresses to paleoburial in fold–thrust belts: preliminary results from calcite twin analysis in the Outer Albanides, *Tectonophysics* 475, 128–141, 2009.
- Lacombe, O.: Calcite twins, a tool for tectonic studies in thrust belts and stable orogenic forelands, *Oil & Gas Science and Technology–Revue d’IFP Energies nouvelles*, 65(6), 809-838, 2010.
- 400 Lacombe O., Tavani S. and Soto R. : Into the deformation history of folded rocks, Special Issue, *Tectonophysics*, 576–577, 1-3, 2012.
- Masaferro, J. L., Bulnes, M., Poblet, J., Eberli, G. P., 2002. Episodic folding inferred from syntectonic carbonate sedimentation: the Santaren anticline, Bahamas foreland, *Sedimentary Geology*, 146, 11-24
- Mazzoli, S., Deiana, G., Galdenzi, S. and Cello, G.: Miocene fault-controlled sedimentation and thrust propagation
405 in the previously faulted external zones of the Umbria-Marche Apennines, Italy, *EGU Stephan Mueller Special Publication Series*, 1, 195-209, 2002.
- Mottram, C. M., Parrish, R. R., Regis, D., Warren, C. J., Argles, T. W., Harris, N. B. and Roberts, N. M.: Using U- Th- Pb petrochronology to determine rates of ductile thrusting: Time windows into the Main Central Thrust, Sikkim Himalaya, *Tectonics*, 34(7), 1355-1374, 2015.
- 410 Mueller K. and Suppe J.: Growth of Wheeler Ridge anticline, California: geomorphic evidence for fault-bend folding behavior during earthquakes, *Journal of structural geology*, 19, 383-396, 1997.
- Nuriel P., Weinberger R., Kylander-Clark A.R.C, Hacker B.R. and Craddock J.P.:The onset of the Dead Sea transform based on calcite age-strain analyses, *Geology* 45 (7), 587-590, 2017.
- Poblet, J., McClay, K., Storti, F. and Munoz, J.A.: Geometry of syntectonic sediments associated with single-layer
415 detachment folds, *Journal of Structural Geology*, 19, 369-381, 1997.
- Poblet, J. and Hardy, S.: Reverse modelling of detachment folds; application to the Pico del Aguila anticline in the south-central Pyrenees (Spain), *Journal of Structural Geology* 17, 1707-1724, 1995.
- Pueyo, E.L., Millan, H. and Pocoví, A.: Rotation velocity of a thrust: a paleomagnetic study in the External Sierras (Southern Pyrenees), *Sedimentary Geology*, 146, 191-208, 2002.



- 420 Riba, O.: Syntectonic unconformities of the Alto Cardener, Spanish Pyrenees: A genetic interpretation, *Sedimentary Geology*, 15, 213–233, 1976.
- Roberts, N. M. and Walker, R. J.: U-Pb geochronology of calcite-mineralized faults: Absolute timing of rift-related fault events on the northeast Atlantic margin, *Geology*, 44, 531-534, 2016.
- Roberts, N. M. W., Drost, K., Horstwood, M. S. A., Condon, D. J., Chew, D., Drake, H., Milodowski, A. E.,
425 McLean, N. M., Smye, A. J., Walker, R. J., Haslam, R., Hodson, K., Imber, J., Beaudoin, N. and Lee, J. K.: Laser ablation inductively coupled plasma mass spectrometry (LA-ICP-MS) U–Pb carbonate geochronology: strategies, progress, and limitations, *Geochronology*, 2, 33-61, 2020.
- Roberts, N. M., Žák, J., Vacek, F. and Sláma, J.: No more blind dates with calcite: Fluid-flow vs. fault-slip along the Očkov thrust, Prague Basin, *Geoscience Frontiers*, 12(4), 101143, 2021.
- 430 Rocher, M., Lacombe, O., Angelier, J. and Chen H.W. : Mechanical twin sets in calcite as markers of recent collisional events in a fold-and-thrust belt: evidence from the reefal limestones of southwestern Taiwan, *Tectonics* 15, 984–996, 1996.
- Rocher, M., Lacombe, O., Angelier, J., Deffontaines, B. and Verdier, F. : Cenozoic folding and faulting in the south Aquitaine Basin (France): insights from combined structural and paleostress analyses, *J. Struct. Geol.* 22, 627–645,
435 2000.
- Rolland, A., Toussaint, R., Baud, P., Schmittbuhl, J., Conil, N., Koehn, D., Renard, F. and Gratier, J.-P.: Modeling the growth of stylolites in sedimentary rocks, *Journal of Geophysical Research: Solid Earth*, 117, B06403, 2012.
- Roure, F., Swennen, R., Schneider, F., Faure, J.L., Ferket, H., Guilhaumou, N., Osadetz, K., Robion, P. and Vandeginste, V.: Incidence and importance of tectonics and natural fluid migration on reservoir evolution in
440 foreland fold-and-thrust belts, *Oil & Gas Science and Technology*, 60, 67–106, 2005.
- Sassi, W., Guiton, M., Leroy, Y.M., Kallel, N., Callot, J.P., Daniel, J.M., Lerat, O. and Faure, J.L.: Constraints on mechanical modelling of folding provided by matrix deformation and fracture network analysis: The case of Split Mountain (Utah, USA), *Tectonophysics*, 576-577, 197-215, 2012.
- Schmittbuhl, J., Renard, F., Gratier, J. P. and Toussaint, R. : Roughness of stylolites: implications of 3D high
445 resolution topography measurements, *Phys Rev Lett*, 93, 238501, 2004.
- Schneider, S., Hammerschmidt, K. and Rosenberg, C. L.: Dating the longevity of ductile shear zones: Insight from $^{40}\text{Ar}/^{39}\text{Ar}$ in situ analyses. *Earth and Planetary Science Letters*, 369, 43-58., 2013.
- Storti, F. and Poblet, J.: Growth stratal architectures associated to decollement folds and fault-propagation folds. Inferences on fold kinematics, *Tectonophysics*, 282(1-4), 353-373, 1997.



- 450 Suppe, J., Chou, G.T. and Hook, S.C.: Rates of folding and faulting determined from growth strata. In: McClay, K.R. (Ed.), *Thrust Tectonics*. Chapman & Hall, Suffolk, pp.105-121, 1992.
- Tavani, S., Storti, F., Lacombe, O., Corradetti, A., Muñoz, J. and Mazzoli, S.: A review of deformation pattern templates in foreland basin systems and fold-and-thrust belts: Implications for the state of stress in the frontal regions of thrust wedges, *Earth-Science Reviews*, 141, 82-104, 2015.
- 455 Tavani S., Storti F., Fernández O, Muñoz JA and Salvini F.: 3-D deformation pattern analysis and evolution of the Añisclo anticline, southern Pyrenees, *Journal of structural geology* 28 (4), 695-712, 2006.
- Tavani S., Storti F., Salvini F. and Toscano C.: Stratigraphic versus structural control on the deformation pattern associated with the evolution of the Mt. Catria anticline, Italy, *Journal of Structural Geology* 30 (5), 664-681, 2008.
- Tavani S., Mencos J., Bausà J. and Muñoz JA.: The fracture pattern of the Sant Corneli Bóixols oblique inversion
460 anticline (Spanish Pyrenees), *Journal of Structural Geology* 33 (11), 1662-1680, 2011.
- Toussaint, R., Aharonov, E., Koehn, D., Gratier, J. P., Ebner, M., Baud, P., Rolland, A., and Renard, F.: Stylolites: A review, *Journal of Structural Geology*, 114, 163-195, 2018.
- Varga, R.J.: Rocky Mountain foreland uplifts: products of a rotating stress field or strain partitioning? *Geology*, 21, 1115-1118, 1993.
- 465 Vermeesch, P.: Unifying the U–Pb and Th–Pb methods: joint isochron regression and common Pb correction, *Geochronology*, 2, 119-131, 2020.
- Weil, A.B. and Yonkee, W.A.: Layer-parallel shortening across the Sevier fold-thrust belt and Laramide foreland of Wyoming: spatial and temporal evolution of a complex geodynamic system, *Earth and Planetary Science Letters*, 357-358, 405-420, 2012.
- 470 Yamato, P., Kaus, B. J., Mouthereau, F. and Castellort, S.: Dynamic constraints on the crustal-scale rheology of the Zagros fold belt, Iran, *Geology*, 39, 815-818, 2011.
- Wang Y., Zwingmann H., Zhou L., Lo C.-H., Viola G. and Hao J.: Direct dating of folding events by $^{40}\text{Ar}/^{39}\text{Ar}$ analysis of synkinematic muscovite from flexural-slip planes, *Journal of Structural Geology*, 83, 46-59, 2016.
- 475 **Dataset availability** : Data either are available as supplementary material or come from properly cited literature.

Author contribution: Conceptualization : O. Lacombe, N. Beaudoin; Data acquisition : all authors; Visualization : O. Lacombe, N. Beaudoin, G. Hoareau, A. Labeur; Funding acquisition : N. Beaudoin; Writing – original draft preparation : O. Lacombe, N. Beaudoin; Writing – review and editing : O. Lacombe, N. Beaudoin, G. Hoareau, J.P. Callot

- 480 **Competing interest** : “The authors declare that they have no conflict of interest”

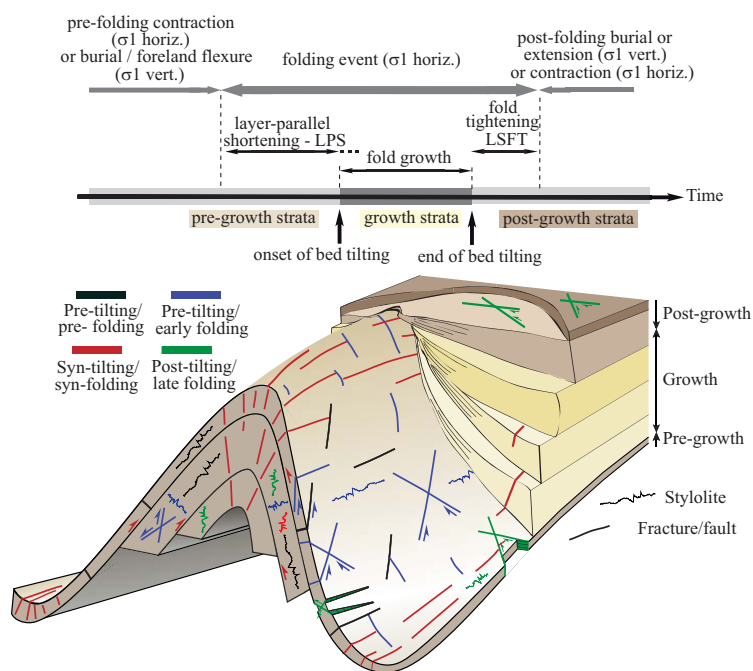


Fig.1. Concept of folding event and associated mesostructures and growth strata.

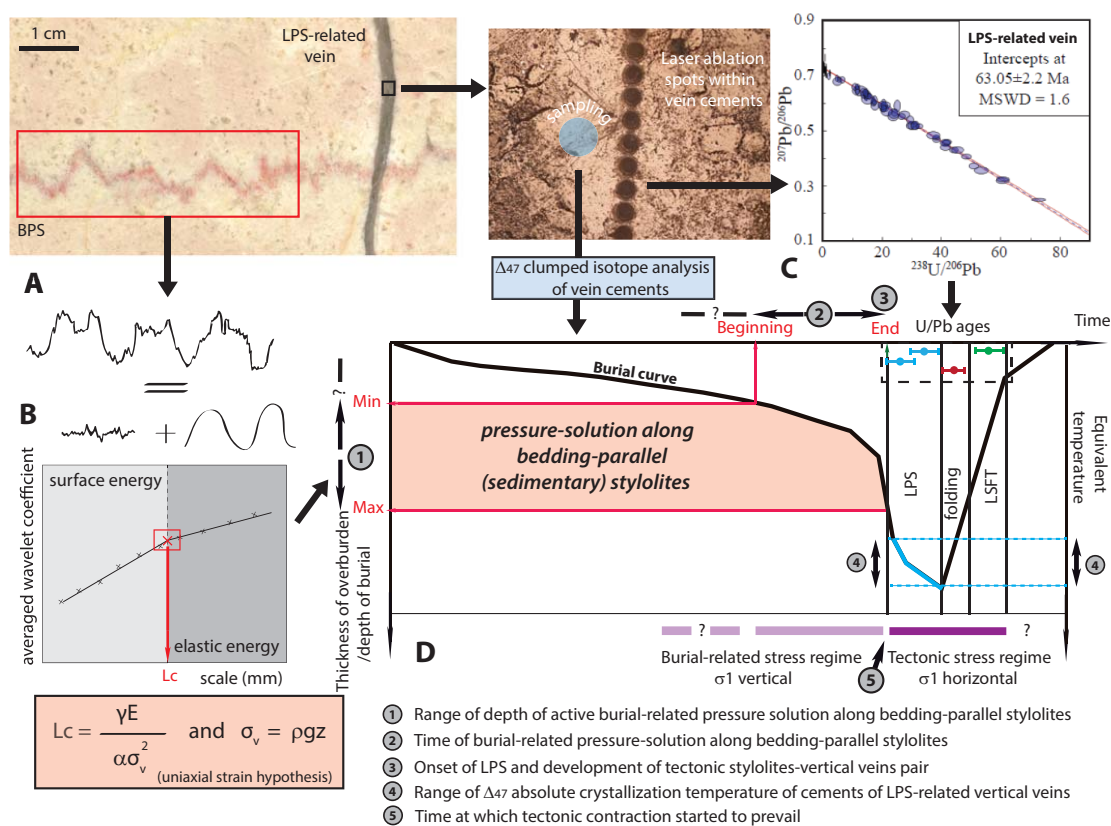


Fig.2. Principle of dating of mesostructures related to the folding event. A. Photograph of a sedimentary stylolite cut by a vertical vein related to layer-parallel shortening (LPS). B. Principle of dating calcite veins using LA-ICP-MS, with laser ablation spots and final Tera-Wasserburg diagram. C. Principle of inversion of the roughness of sedimentary stylolites for stress. σ_v is the vertical stress, $\alpha = ((1-2\nu) * (1+\nu)^2) / (30\pi(1-\nu)^2)$, γ is the solid-fluid interfacial energy, ν is the Poisson ratio, E is the Young modulus, ρ is the dry density, g is the gravitational field acceleration and z is the depth. D. Principle of the combination of U-Pb dating and absolute $\Delta 47$ thermometry of calcite cements (here for LPS-related veins) with maximum depth of burial-related dissolution from sedimentary stylolites and burial-time evolution of strata to derive the timing of deformation stages during the folding event.

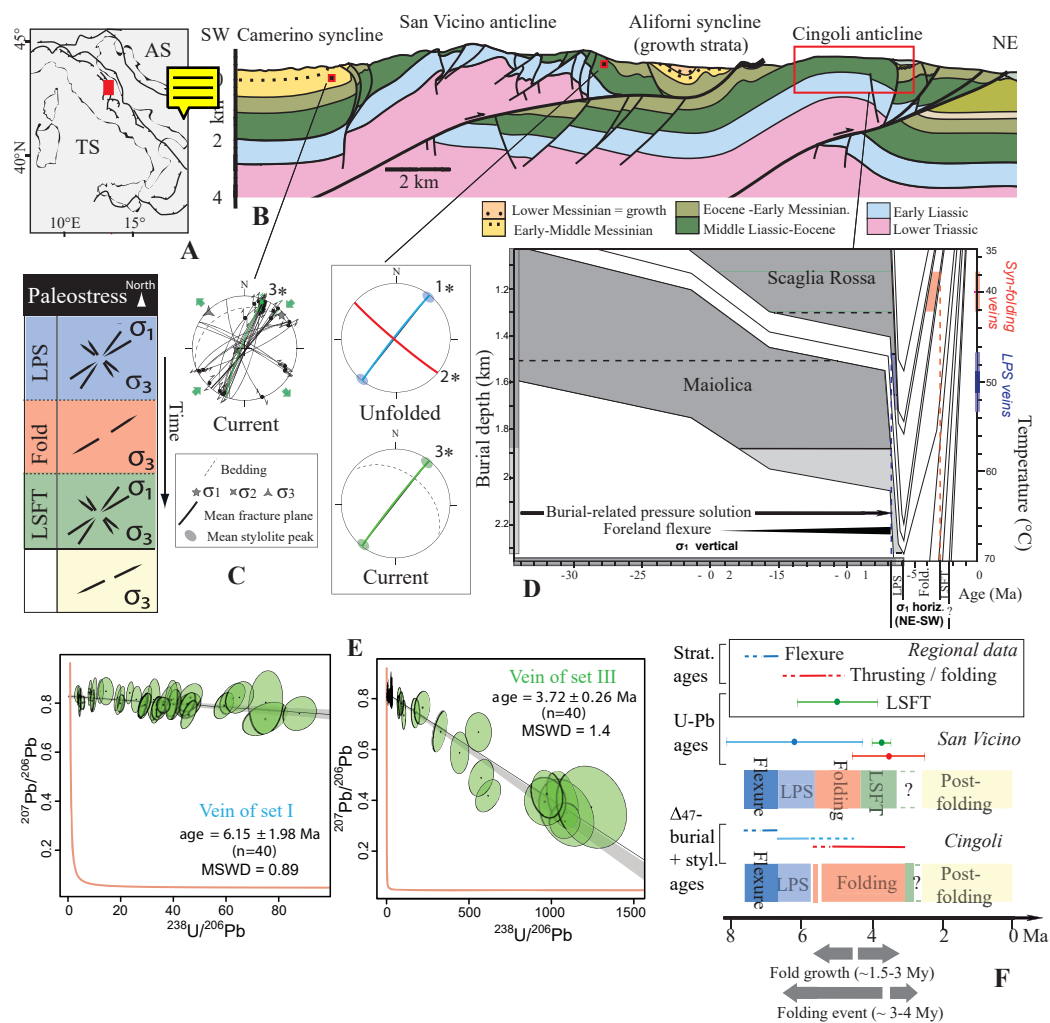


Fig.3. San Vicino and Cingoli anticlines: A: location (AS: Adriatic Sea; TS: Tyrrhenian sea). B: cross section (after Mazzoli et al., 2002). C: Orientation of the main sets of mesostructures (relative chronology, 1 to 3), reported in current or unfolded attitude on a lower hemisphere Schmidt stereonet, and associated paleostress evolution. * denotes mesostructures dated using U-Pb. D: Burial model of Cingoli constructed considering thickness from stratigraphic and well data corrected for chemical and physical compaction (modified from Labeur et al., 2021). The range of depths reconstructed from sedimentary stylolite roughness inversion (with uncertainty shaded in light grey) are reported for each formation as grey levels. The results of clumped isotope analysis (i.e., temperatures of precipitation of vein cements at thermal equilibrium with the host rock) are reported for LPS-related veins (blue) and syn-folding veins (red). The deduced timing of the deformation stages is reported. E: Age dating results for veins from San Vicino anticline: Tera-Wasserburg concordia plots for carbonate samples showing $^{238}\text{U}/^{206}\text{Pb}$ vs $^{207}\text{Pb}/^{206}\text{Pb}$ for veins of sets I (LPS-related) and III (LSFT-related) (n—no. of spots). MSWD—mean square of weighted deviates. F: Timing and duration of deformation stages. Regional data are from Mazzoli et al., 2002 (flexure), Calamita et al. 1994 (folding and thrusting), Beaudoin et al., 2020c (LSFT). Color code for C and F: dark blue: flexure-related extension. blue: layer-parallel shortening (LPS); red: fold growth; green: late stage fold tightening (LSFT); yellow: post-folding extension.

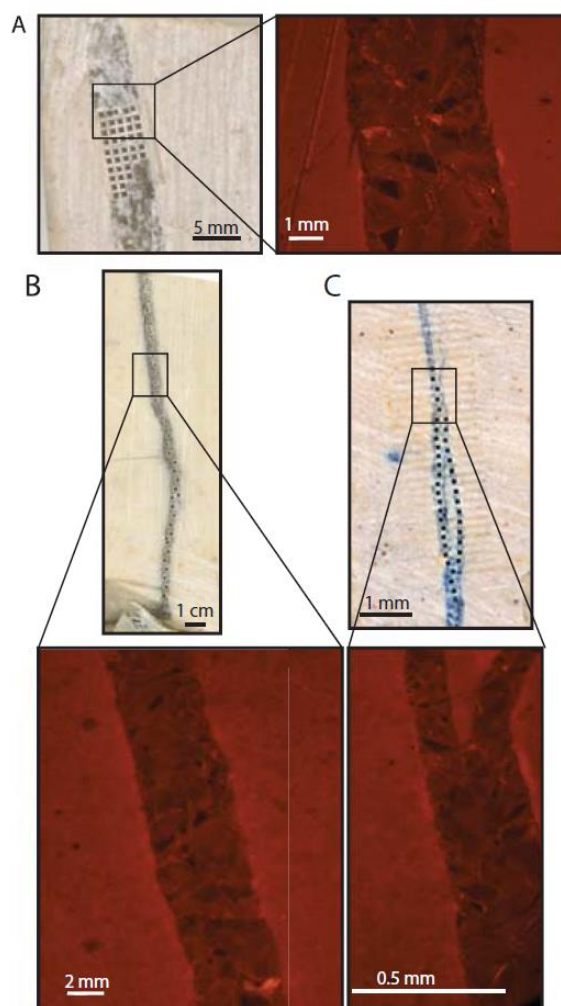


Fig.4. 2D scans of veins dated by LA-ICP-MS U-Pb geochronology from San Vicino anticline, with location of the ablation spots and diagenetic state observed under cathodoluminescence microscopy. a) sample A16 (LPS-related vein), b) sample A19 (syn-folding vein), c) sample A20 (LSFT-related vein).

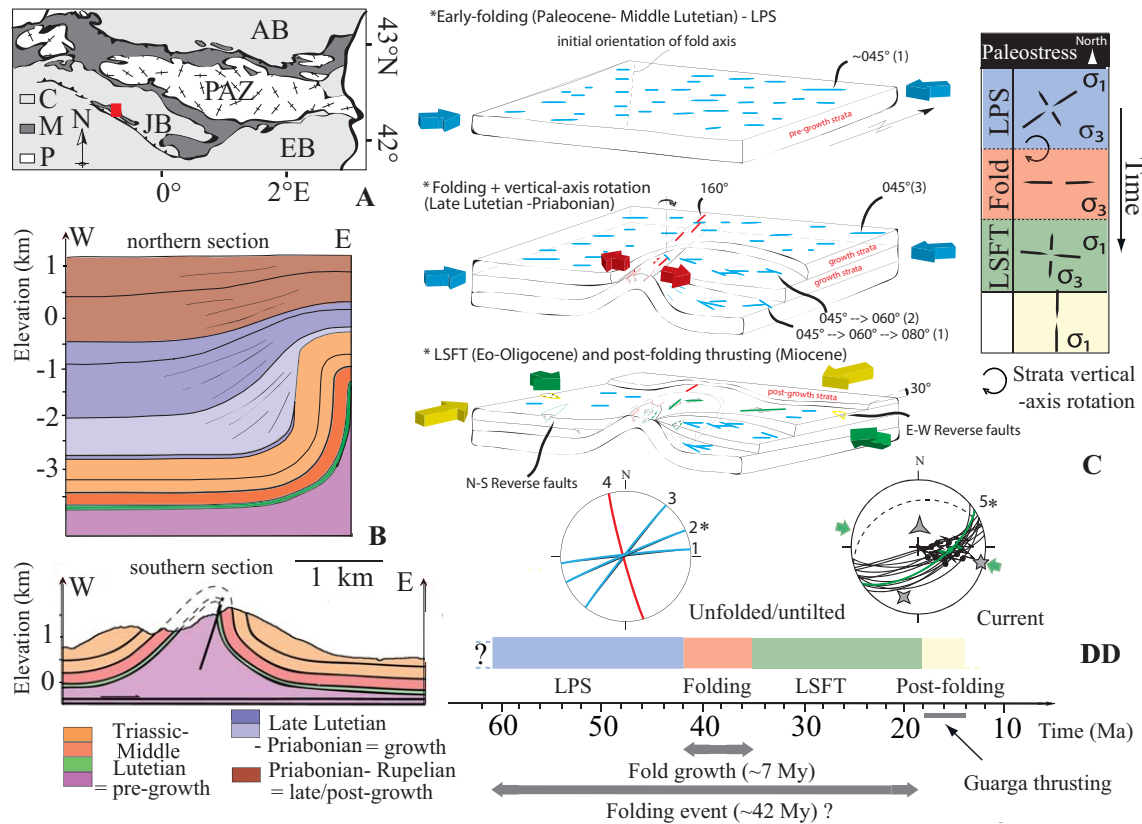


Fig.5. Pico del Aguila anticline: A: location (AB: Aquitaine Basin, JB: Jaca Basin, EB: Ebro Basin, PAZ: Pyrenean Axial Zone; P: Paleozoic; M: Mesozoic; C: Cenozoic). B: cross sections (north after Poblet et al., 1997, south after Beaudoin et al., 2015). C: Orientation of the main sets of mesostructures (relative chronology, 1 to 5), reported in current or unfolded attitude on a lower hemisphere Schmidt stereonet (same key as Fig.3), and associated structural and paleostress evolution. Block diagrams modified after

Beaudoin et al. (2015). * denotes mesostructures dated using U-Pb. D: Timing and duration of deformation stages. Color code for C and D: blue: layer-parallel shortening (LPS); red: fold growth; green: late stage fold tightening (LSFT); yellow: post-folding compression.

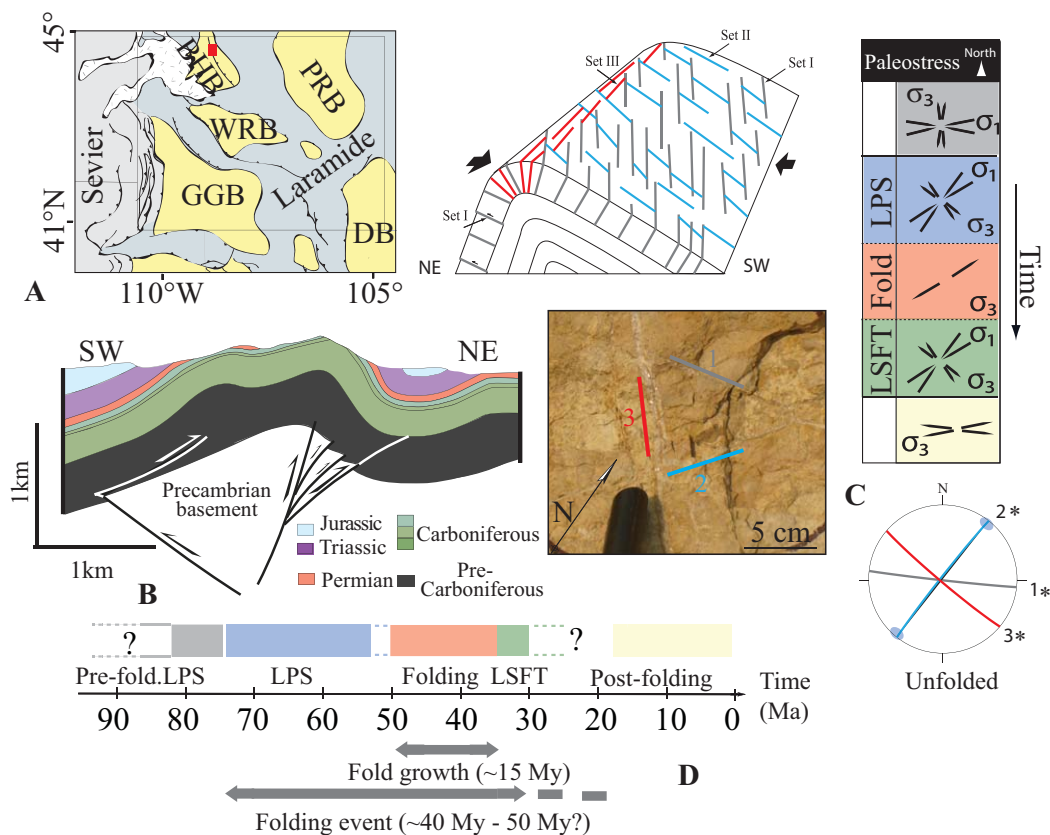


Fig.6. Sheep Mountain anticline: A: location (BHB: Bighorn Basin; WRB: Wind River Basin; PRB: Powder River Basin; GGB: Greater Green River Basin; DB: Denver Basin). B: cross section (after Amrouch et al., 2010); C: Orientation of the main sets of veins (relative chronology, 1 to 3), shown on a field photograph and on a block-diagram of the final fold geometry, reported in unfolded attitude on a lower hemisphere Schmidt stereonet (same key as Fig.3), and associated structural and paleostress evolution. * denotes mesostructures dated using U-Pb. D: Timing and duration of the deformation stages. Color code for C and D: grey: pre-folding layer-parallel shortening kinematically unrelated to folding; blue: layer-parallel shortening (LPS); red: fold growth; green: late stage fold tightening (LSFT); yellow: post-folding extension.

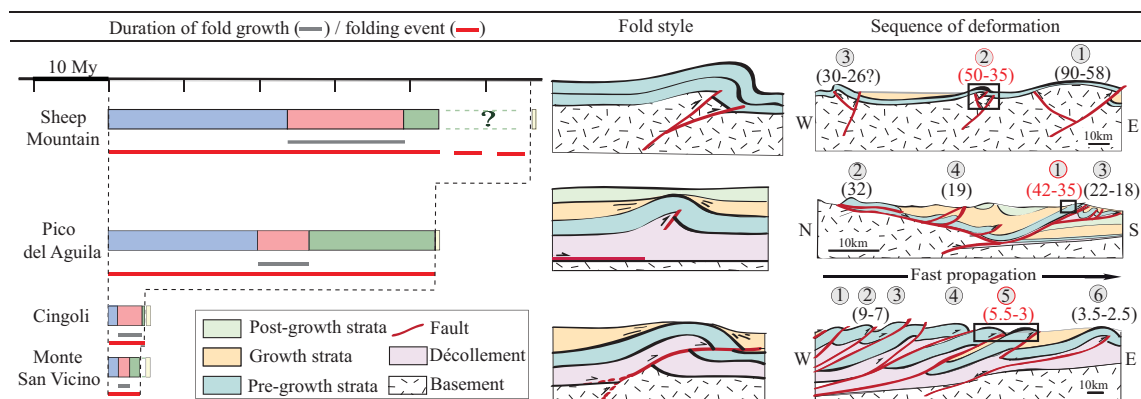


Fig.7. Compared durations of the stages of the folding event, fold style (= final fold geometry) and sequence of regional deformation for the four studied folds (circled numbers 1 to 6 : order of structural development, i.e., sequence of folding/thrusting, with corresponding ages in Ma (between parentheses), red : from this study; black : from the literature (Beaudoin et al., 2018 for Wyoming, Jolivet et al. 2007 for the Pyrenees, Calamita et al., 1994 and Curzi et al., 2020 for the Apennines). Color code: blue: layer-parallel shortening (LPS); red: fold growth; green: late stage fold tightening (LSFT); yellow: post-folding extension/compression.